environments

Article

Molecular Structure of the Humic Acids Isolated from Organic Material from Modern and Paleosoils (MIS 5e and MIS 7) of Batagay Megaslump Ice Complex Deposits (Yakutia, Russia)

Vyacheslav Polyakov [1,*], Alexey Lupachev [2], Evgeny Abakumov [1] and Petr Danilov [3]

[1] Department of Applied Ecology, Faculty of Biology, St. Petersburg State University, Universitetskaya Embankment, 7/9, St. Petersburg 199034, Russia; e.abakumov@spbu.ru
[2] Institute of Physico-Chemical and Biological Problems in Soil Science, Russian Academy of Sciences, Institutskaya St., 2/2, Pushchino 142290, Russia; a.lupachev@gmail.com
[3] Prof. D.D. Savvinov Science Research Institute of Applied Ecology of the North, M.K. Ammosov North-East Federal University, Yakutsk 677007, Russia; danpp@mail.ru
* Correspondence: v.polyakov@spbu.ru; Tel.: +7-9531724997

Abstract

The degradation of modern and ancient permafrost-affected soils and organic-rich sediments and the release of relict soil organic matter from the frozen state are critical for understanding the global carbon cycle in a changing climate. The molecular structure of humic acids isolated from modern Cryosols and paleosoils from the Ice Complex deposits in the Batagay megaslump area was investigated. The elemental composition analysis was performed using a CHN analyzer, and molecular composition analysis was determined by CP/MAS ^{13}C-NMR spectroscopy. Analysis of the molecular structure of humic acids showed that MIS 5e paleosoils are characterized by a relatively high content of aliphatic structural fragments (C,H-AL—29–36%) and a low content of aromatic structural fragments (AR/AL—0.49–0.43), which reveals low humification rates in this time period. The composition of humic acids from MIS 7 paleosoils shows a relatively high content of aromatic structural fragments compared to modern soils (AR/AL—0.47) and MIS 5e deposits (AR/AL—0.67–0.54), indicating a longer humification process in heterogenic conditions (warm and cold periods). The results indicate that the molecular structure of humic acids is a dynamic parameter of the environment that reflects the local conditions of pedogenesis and organic matter formation. Permafrost thawing leads to the release of organic matter (including matter that is relatively weakly resistant to biodegradation where aliphatic structural fragments dominate the composition of humic acids) that may strengthen the emission of climate-active gases into the atmosphere and boost climate change.

Keywords: humic acids; ^{13}C NMR spectroscopy; permafrost; Ice Complex; Cryosols

check for updates

Academic Editor: Joaquim Esteves Da Silva

Received: 27 June 2025
Revised: 6 August 2025
Accepted: 14 August 2025
Published: 15 August 2025

Citation: Polyakov, V.; Lupachev, A.; Abakumov, E.; Danilov, P. Molecular Structure of the Humic Acids Isolated from Organic Material from Modern and Paleosoils (MIS 5e and MIS 7) of Batagay Megaslump Ice Complex Deposits (Yakutia, Russia). *Environments* **2025**, *12*, 282. https://doi.org/10.3390/environments12080282

Copyright: © 2025 by the authors. Licensee MDPI, Basel, Switzerland. This article is an open access article distributed under the terms and conditions of the Creative Commons Attribution (CC BY) license (https://creativecommons.org/licenses/by/4.0/).

1. Introduction

The global carbon pool (in the top 1 m) in soils is estimated at approximately 1500–1600 Gt [1], including 400–500 Gt of carbon stored in permafrost [2]. Under climate change and landscape transformation, the release of carbon from permafrost could play a significant role in atmospheric carbon fluctuations [3]. Most of the released soil organic matter (SOM) is absorbed by the atmosphere and oceans and sequestered by soils and plants [4]. However, direct carbon balance calculations indicate the existence of a "missing carbon sink" which may be linked to carbon conservation, its qualitative composition, as

well as redistribution and redeposition of organic matter [5]. Thermoerosion and slump formation processes in permafrost-affected environments and the release of SOM from thawing permafrost are among the key components of the Arctic carbon cycle [6].

Coastal erosion along small and large riverbanks, as well as in Arctic coastal regions, releases approximately 8–15 Tg C-CO_2 yr^{-1} of SOM [7]. According to Nielsen et al. [8], by 2100, the rate of carbon release from permafrost could increase by 1.5 times, leading to significant inputs of SOM into Arctic seas. In addition to coastal erosion, thermokarst processes, driven by the thawing of ice-rich Late Pleistocene permafrost Ice Complex deposits, contribute to carbon emissions, releasing 19–58 Tg C-CO_2 yr^{-1} [9]. Eroding landscapes are a key source of bioavailable carbon, as dissolved organic matter can be readily utilized by microorganisms [10]. The formation of Ice Complex deposits is linked to the rapid accumulation of labile carbon and its subsequent preservation under conditions of synlithogenic pedogenesis that took place in the Late Pleistocene, the simultaneous mineral material deposition, its pedogenic reworking and further transition into the frozen state due to aggrading permafrost [11,12], making it a formation for long-term carbon storage [13]. The Ice Complex covers over 1 million km^2 in northeastern Siberia, Alaska, and Canada [14] and contains 657 $\pm$ 97 Gt of carbon [15]. A critical question in permafrost degradation is the susceptibility of organic matter to biodegradation [16]. While Knoblauch et al. [17] found no significant differences between the organic matter properties of the Ice Complex organo-mineral deposits and early Holocene deposits, other studies suggest that Ice Complex deposits formed under relatively more aerobic conditions and may be more vulnerable to decomposition than those formed in the early Holocene [15].

Since the 1970s, a retrogressive thaw slump (RTS) known as "Batagayka" or Batagay megaslump, has been forming in the Yana Highlands of northeastern Siberia. Today, it is recognized as the largest RTS on Earth [18]. There is a significant gap in research focused on Pleistocene pedogenesis in the Yana Plateau region. Some studies briefly mention "pedogenic" characteristics in the composition and features of the examined deposits, often based solely on the darker coloration of specific subhorizontal layers within the deposit sequence [11,19]. The morphology and properties of modern Cryosols in the area have been addressed in a few publications [20]. Just recently, in [21], a profound study of the microstructure and geochemical properties of modern and buried soils and hosting permafrost sediments of the Batagay RTS was published where we attempted to characterize the degree and peculiar properties of pedogenic transformation of the Batagay RTS deposits.

Permafrost degradation here is occurring at a rate of 1 million m^3 per year, releasing 4000–5000 tons of organic matter annually [18]. Further expansion of the Batagay megaslump could increase the mobilization of organo-mineral sediments [22], potentially affecting atmospheric CO_2 levels [23]. Thus, it is crucial to assess the resistance of organic matter to biodegradation, as this will help refine existing carbon-balance models for northwestern Siberia.

One method for assessing the qualitative composition of organic matter is ^{13}C-NMR spectroscopy of humic acids (HAs) [24]. This approach helps determine the content of environmentally stable HA fragments [25] and is widely used to evaluate the stabilization rates of SOM in the Arctic [26–28]. The hypothesis of this study is that organic matter accumulated during the Late Pleistocene synlithogenic pedogenesis exhibits varying degrees of resistance to biodegradation, depending on the bioclimatic conditions of the Ice Complex formation. The aim of this study is to evaluate the degree of resistance to biodegradation of organic matter released from the Batagay megaslump. To achieve this, the major task of the study has been defined—to analyze the molecular properties of the organic matter of modern and ancient soils and to estimate its resistivity to biodegradation.

2. Materials and Methods

2.1. The Study Area

Batagay RTS, placed in northern Yakutia, measures roughly 1 × 2 km, with the main wall of the exposure extending over 1.6 km (Figure 1). A stratigraphic sequence of frozen deposits exceeds 80 m in thickness, covering a time span from 250 to approximately 600–700 Kyr (as estimated through various research methods [29]). The Batagay RTS (67.58° N, 134.77° E), located in 10 km southeast of the Batagay settlement in Sakha (Yakutia, Russia), began to develop from a series of thermal erosion gullies at the end of the 1960s [19] with a gradual increase in the rate of degradation. By 2015, it reached the width of 840 m with an overall area of more than 70 ha [12,30]. Then, the rate of the retreat of the exposure's walls somewhat slowed [31]. Presently, the maximum width is about 1 km [18]. The Batagay RTS is found in the Kirgillyakh-Khatyngnakh saddle, mainly between 260 and 330 m a.s.l. This area has a sharply continental climate of the subarctic zone [32]. The mean annual air temperature is –11.6 °C, and the annual precipitation is 210 mm. The region belongs to the zone of continuous permafrost with a thickness of about 300 m, and the mean annual ground temperature in the upper part of the permafrost varies from –5.5 to –7.0 °C [32]. The thickness of the active layer varies from 0.6–0.8 to 1.4–1.6 m depending on the soil-vegetation cover [33]. The permafrost section consists of disperse sediment units underlain by metamorphosed slate bedrock of the Triassic period [12] appearing on the surface only in the deepest parts of the section and in the streambeds of springs inside the slump.

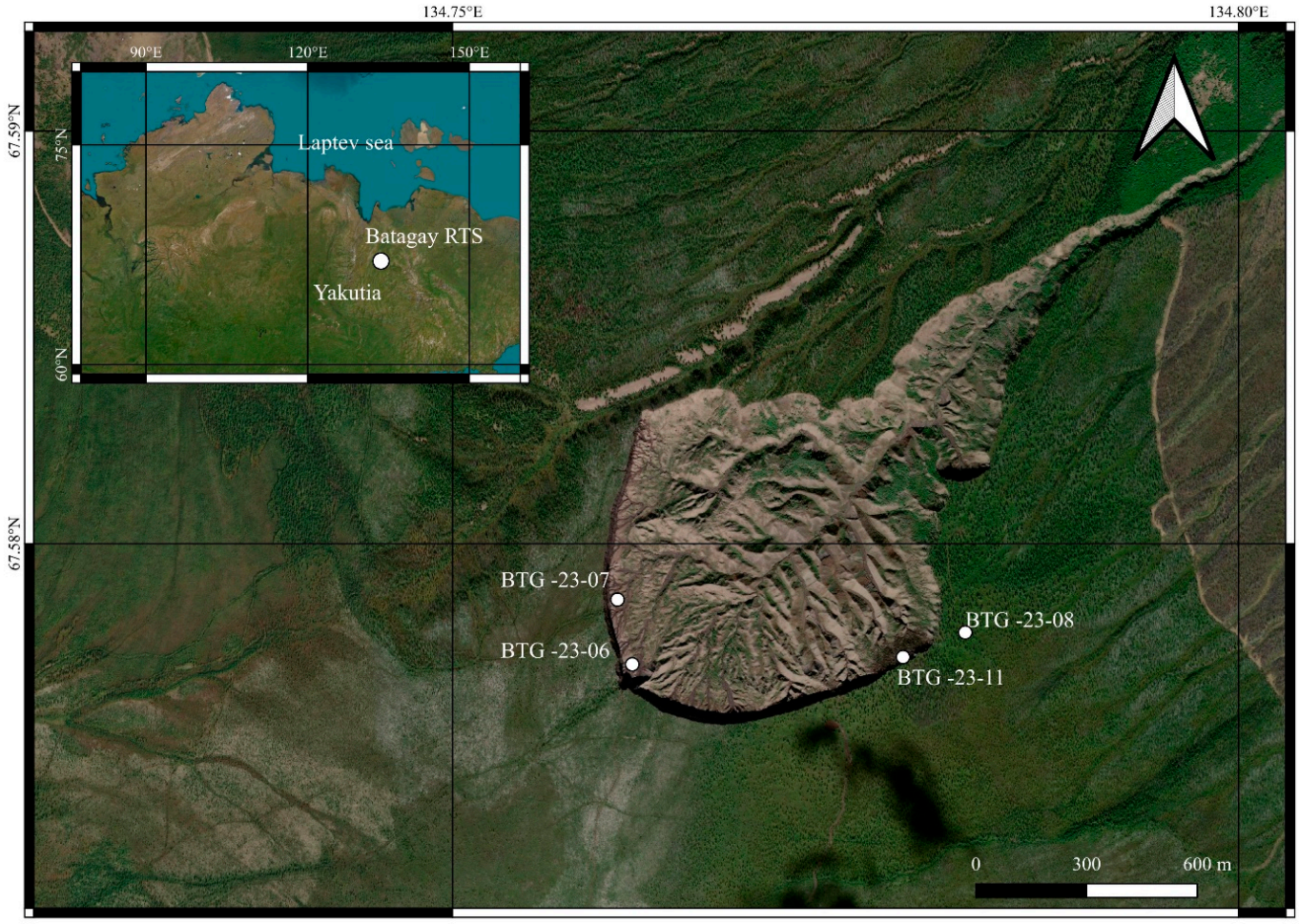

(**a**)

Figure 1. *Cont.*

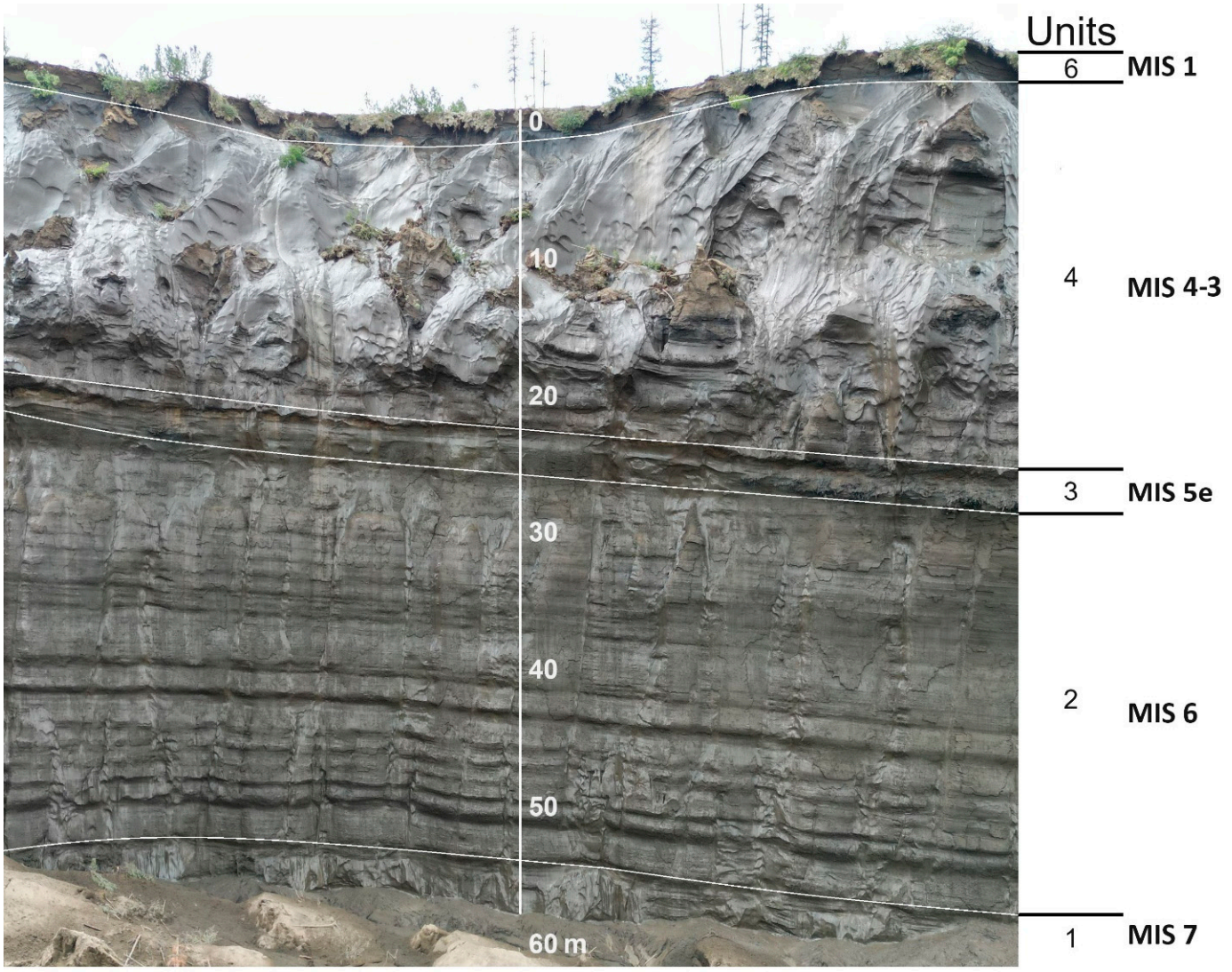

(**b**)

Figure 1. The study area. Batagay RTS. Geographical location (**a**) and headwall structure adjacent to BTG-23-06 and BTG-23-07 sampling points (**b**).

Northern taiga larch woodlands with admixtures of silver birch and, less frequently, aspen predominate on the Yana Plateau [31,34]. The ground cover is mainly represented by lichens, mosses, and some grasses [35]. With altitude, larch woodlands are replaced by thickets of Siberian dwarf pine or mountain tundra.

Modern soils of forest watersheds and gentle slopes are predominantly represented by sandy loamic Histic Spodic Cryosols underneath larch woodlands. These soils have a well-developed upper peat horizon of about 10 cm in thickness, under which a mineral horizon with an ooid ("caviar-like") postcryogenic soil structure is located. The middle-profile mineral soil horizons have slightly pronounced signs of gleyzation and ferrugination, as well as migration of organic compounds. Suprapermafrost horizons are often waterlogged and structureless.

The structure and physicochemical properties of the Batagay RTS modern soil, hosting sediments and paleosoils are thoroughly discussed in the recent paper [21], which is the basis for our assumptions about the environment in the most favorable epochs for the development of pedogenic processes.

2.2. Sampling Strategy

Buried soils and soil-like bodies were studied during field research in 2023 and 2024 field seasons, both in individual accessible areas of the frozen walls of the Batagay RTS exposure. Modern and paleosoils were named in accordance with IUSS Working Group WRB [36]. The term "cryopedolith" (proposed by S.V. Gubin [37,38]) or "soil-like body" refers to a sediment unit that has undergone initial pedogenesis alongside syngenetic freezing and intense accumulation of mineral material. This material was deposited primarily through eolian processes under relatively cold and arid conditions, though other reworking mechanisms may have contributed. Both the lower and upper sand units in the Batagay megaslump wall structure represent cryopedoliths (soil-like bodies) and contain the least pedogenically altered material within the entire stratigraphy. Syngenetic pedogenesis occurred simultaneously with mineral deposition and incremental permafrost aggradation during glacial periods, resulting in distinct pedogenic features. However, this process did not lead to the formation of fully developed (e.g., epigenetic) soil profiles.

Modern and buried soils, as well as permafrost soil-like bodies, were sampled using standard soil-science methods to characterize the structure and properties of units within the Batagay megaslump stratigraphic sequence. From each distinct soil horizon or sedimentary unit, samples (200–300 g) were collected from both the frozen exposure wall and borehole cores. These samples were air-dried, manually ground into a homogeneous mass, and sieved through a 1 mm mesh to remove large plant residues and coarse mineral fractions. Thus, the obtained "median" samples can be considered as representative of the spatial and property variability of the sampled sedimentary units following established protocols for permafrost studies [2]. Each soil horizon was sampled in field triplicate, constituting the bulk sample afterwards. The analysis of the elemental composition of HAs was carried out in three repetitions. Low coefficients of variation (<5% for elemental composition of HAs) confirmed homogeneity within units. Our sample numbers align with or exceed those in similar studies of Ice Complex deposits [18].

The first sampled interval is confined to the lower part of the section (66–70 m) composed of sediments of the lower Ice Complex (BTG-23-06; MIS 7 (approx. 220 Kyr) or possibly MIS 15–17 (approx. 650 Kyr)) and is marked in the wall by a paleosoil, which is morphologically close to modern Histic Gleyic Cryosol. An abundance of coarse plant remains, their layered bedding, abrupt boundaries between organic interlayers and underlying mineral sediments, as well as intense gleyization of the mineral sandy loamic part of paleosol and the high ice content (massive-agglomerate, lens-type, and reticular cryostructures) allow us to suppose that during the formation of this part of the section, the surface was significantly waterlogged and contained intrapolygonal water pools and a thick (in some cases, possibly, subaqueous) peat cover forming between ice wedges.

The second sampled paleosoil, which is most distinct in terms of morphological and physicochemical properties of the material, is allocated to a subhorizontal interlayer of the epigenetic (formed under conditions of a relatively weak or absent deposition of mineral sediment) buried soil located in the central part of the outcrop at a depth of 38–43 m (BTG-23-11, BTG-23-07; MIS 5e (approx. 130 Kyr)). The morphological features of the material are close to the modern sandy loamic Histic Spodic Cryosols. The processes of migration of Al–Fe humic compounds are clearly seen in the ocherous color of mineral horizon under the organomineral layer. Clearly formed crumb–platy and ooidal aggregates, well-preserved charcoal particles, and root channels are clearly visible in the microstructure; soil pores have distinct boundaries. Mineral particles are covered by thin light brown films of iron oxides; some poorly rounded mineral grains contain clods of dark organic material on the surface. Optically unoriented clay participates in the formation of complex microaggregates.

Samples were collected from key stratigraphic units (MIS 5e, MIS 15–17) representing characteristic Ice Complex deposits; these deposits are well dated and are characteristic of Northeastern Siberia [11,15]. The samples of modern soils correspond to those that are developing in Northeastern Yakutia [20].

The descriptions of studied soil and soil-like bodies are presented in Table 1.

Table 1. The descriptions of studied samples of soil and soil-like bodies.

ID	Index	Marine Isotope Stage	Horizon	Depth	Location	Name (WRB [36])
1 2	BTG-23-08	Modern soil	He Bh	1–9 cm 9–50 cm	Undisturbed soil, formed to the east relatively from Batagay RTS. Histic Cryosol. N 67.578406, E 134.783202	Histic Cryosol
3 4 5	BTG-23-11 BTG-23-07	MIS 5e	[He] [Bs] [He]	20–25 m	Buried paleosol. Histic Gleyic Cryosol. N 67.577686, E 134.777580 (BTG-23-11), N 67.578988, E 134.762130 (BTG 23-07)	Buried Histic Spodic Cryosol Paleoerosional cuts
6 7 8	BTG-23-06	MIS 7 or 15-17	[O] [He] [Bl]	More than 60 m	Visible foot of the Ice Complex. Histic Gleyic Cryosol. N 67.577284, E 134.762860	Buried Histic Reductaquic Cryosol

2.3. Laboratory Methods

The pH values were measured potentiometrically in aqueous suspensions. Total carbon and nitrogen contents were determined using a CHN analyzer (EA3028-HT EuroVector, Pavia, Italy) with an analytical accuracy of ±0.01 mg or ±0.5% RSD for carbon and ±0.02 mg or ±0.5% RSD for nitrogen. Particle size distribution was analyzed by the sedimentation method. Phosphorus (reported as P_2O_5) and potassium (reported as K_2O) contents were measured using the Kirsanov method [39]. HAs were extracted from the soil samples following the standardized procedure recommended by the International Humic Substances Society (IHSS), incorporating modifications introduced by Vasilevich et al. [40]. The elemental composition of humic substances was determined as the percentage content of carbon (C), hydrogen (H), nitrogen (N), and oxygen (O). All elemental data were corrected for residual moisture and ash content. The modified Van Krevelen diagram was employed for graphical interpretation of the elemental ratios, providing insights into the structural characteristics and origin of the humic substances. HAs represent the more stable and structurally complex fraction of SOM, with higher molecular weight and aromaticity compared to fulvic acids (FAs) [25]. This makes them a critical indicator of long-term carbon persistence in permafrost regions. HAs dominate the recalcitrant SOM pool in permafrost-affected soils, while more soluble and labile FAs are often rapidly lost by leaching or microbial degradation upon thawing/freezing processes.

The elemental composition (C, H, N) of humic acids (HAs) was determined using a CHNS analyzer (EA3028-HT EuroVector, Pavia, Italy). Oxygen content was calculated by difference. The obtained elemental ratios were visualized using a Van Krevelen diagram (H/C vs. O/C atomic ratios) to assess the structural characteristics and degree of transformation of the humic substances. Oxygen content was calculated from

$$O = 100 - (C + H + N) \quad (1)$$

where C, H, N content was obtained by CHN analyzer.

The degree of oxidation was calculated from

$$\mathrm{w} = 2 \times ((O/16) - (H/1.01))/(C\,/\,12.01) \quad (2)$$

where C, H content were obtained by CHN analyzer.

Solid-state ^{13}C NMR spectra of humic acids (HAs) were acquired using cross-polarization magic angle spinning (CP/MAS) methodology on a Bruker Avance 500 MHz spectrometer (Billerica, MA, USA) in a 3.2 mm ZrO_2 rotor. The number of scans (NS) was 30,720.

The content of aromatic fragments in the composition of HAs is a qualitative indicator of the resistance of organic matter to biodegradation [25]. This is due to the formation of biochemically more stable organic compounds relative to aliphatic compounds [25]. According to Schädel et al. [41], organic matter saturated with aromatic compounds of HAs is less susceptible to microbial decomposition due to the complex ring structure of molecular compounds.

3. Results and Discussion

The analysis of modern soils and paleosoils buried in the Ice Complex deposits revealed relatively similar chemical characteristics. Total nitrogen content in the studied modern soils and paleosoils ranged from 0.05% in lower horizons to 0.28% in upper horizons, suggesting that plant residues constitute the primary nitrogen source. A similar pattern was observed for total carbon content, with maximum values in modern or former superficial horizons (6.05%) sharply decreasing with depth (0.38%). The C/N ratio varied from 7.14 in lower horizons to 21.63 in upper horizons, indicating limited nitrogen availability. This distribution pattern is typical for Arctic soils [42], resulting from short and cold growing seasons and carbon accumulation primarily as coarse humus forms. Ice Complex deposits showed heterogeneous composition, reflecting different stages of organomineral accumulation during complex formation. Total nitrogen content ranged from 0.06% to 1.14% (MIS 7), for MIS 5e—0.24% of N, while total carbon content varied from 0.42% to 20.63% (MIS 7 paleosoil), for MIS 5e—0.24% of C. Analysis of available phosphorus (P_2O_5 mg/100 g) revealed higher concentrations in Ice Complex deposits (MIS 5e and MIS7) compared to modern Cryosols (6.87 vs. 2.71 on average). Potassium content (K_2O mg/100 g) was similar in both (4.7 in Ice Complex vs. 4.6 in soils). pH values were near-neutral (pH—6.6). Thus, paleosoils from Ice Complex deposits show physicochemical parameters similar to those of modern Arctic soils. However, the key remaining question concerns the fate of Ice Complex organic matter in terms of its possible subsequent transformation processes after thawing from ancient permafrost.

Molecular Structure of HAs Isolated from Soils and Relict Organic Matter of the Ice Complex

To analyze intramolecular processes occurring in HA molecules, we conducted an elemental composition analysis of HAs (Table 2). The elemental composition of HAs isolated from soils and paleosoils from the Ice Complex deposits showed that carbon content falls within a narrow range for all studied samples (52.07–56.21%, with a coefficient of variation of 2.69%). Similar consistency was observed for hydrogen and oxygen contents. Hydrogen content varied from 4.61% to 5.39% (coefficient of variation 4.65%), while oxygen content ranged from 37.16% to 41.15% (coefficient of variation 3.49%). The greatest variation was observed in nitrogen content, which ranged from 1.76% (BTG-23-06 [He]; MIS 7) to 3.15% (BTG-23-11 [He]; MIS 5e), with a coefficient of variation of 20.53%. This relatively high variation in nitrogen content is associated with differences in quality of precursors of humification. The vegetation cover and humification conditions varied significantly during different stages of Ice Complex deposit and paleosoil formation, which is reflected in the elemental composition of HAs.

Table 2. The elemental composition of HAs isolated from modern and paleosoils (gravimetric concentration are given for C, H, N. C/N, H/C, O/C—atomic ratio).

ID	Index	Horizon	N, %	C, %	H, %	O, %	C/N	H/C	O/C	w
1	BTG-23-08	He	2.36 ± 0.01	54.91 ± 0.11	5.14 ± 0.19	37.59 ± 0.31	27.16	1.11	0.51	−0.08
2		Bh	2.9 ± 0.06	54.88 ± 0.16	5.04 ± 0.05	37.18 ± 0.19	22.09	1.09	0.51	−0.08
3	BTG-23-11	[He]	3.15 ± 0.03	52.07 ± 0.15	5.17 ± 0.09	39.61 ± 0.21	19.28	1.18	0.57	−0.04
4		[Bs]	2.17 ± 0.15	54.02 ± 2.46	5.39 ± 0.38	38.42 ± 2.92	29.08	1.18	0.54	−0.11
5	BTG-23-07	[He]	2.32 ± 0.05	53.94 ± 0.04	5.15 ± 0.12	38.59 ± 0.14	27.10	1.14	0.54	−0.06
6	BTG-23-06	[O]	1.79 ± 0.11	52.45 ± 0.41	4.61 ± 0.07	41.15 ± 0.55	34.32	1.04	0.59	0.13
7		[He]	1.76 ± 0.03	56.21 ± 0.16	4.87 ± 0.12	37.16 ± 0.28	37.31	1.03	0.5	−0.04
8		[Bl]	2.48 ± 0.07	55.72 ± 0.04	4.94 ± 0.07	36.86 ± 0.11	26.22	1.05	0.5	−0.06

To analyze intramolecular processes, an elemental composition diagram was plotted (Figure 2).

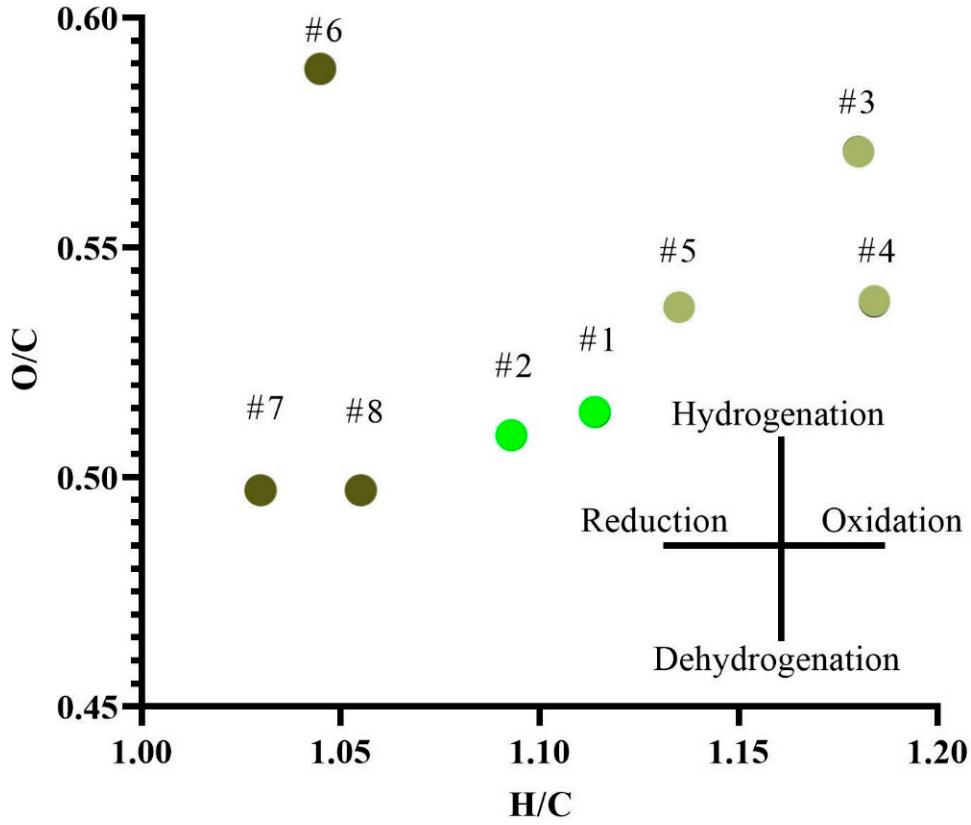

Figure 2. Distribution fields of elemental composition indices in H/C-O/C coordinates of HAs. Green—modern Cryosols; light-brown—MIS 5e deposits; dark-brown—MIS 7 deposits. #1–#8 correspond to Table 2.

The data show that the oxidation index (O/C) values fall within a narrow range for most samples, except for samples #3 (BTG-23-11 [He]) and #6 (BTG-23-06 [O]), indicating an active hydrogenation process where hydrogen molecules attach to carbon molecules. This process may reduce molecular resistance to biodegradation by breaking double and triple bonds in HAs, while increasing their solubility through the formation of hydroxyl groups (-OH). This process can actively develop under anaerobic conditions, taking into account the fact that organic matter has been in a frozen state for a long time in the Ice Complex deposits. It can play a key role in the transformation of intramolecular complexes. According to the H/C index, which reflects the degree of HA saturation

and indicates the maturity of HAs, we can note that the most mature HAs were formed during MIS 7 stage (#6–8), followed by HA samples from modern Cryosols (#1–2), while deposit samples from MIS 5e (#3–5) are characterized as the most labile. According to the ANOVA test, significant differences between groups of modern Cryosols and MIS 5e ($p = 0.01$) and MIS 7 deposits ($p = 0.02$) as well as between MIS 5e and MIS 7 deposits ($p = 0.0006$) have been found. This distribution indicates the heterogeneous formation and transformation of HAs in different time periods, which may be due to both the qualitative composition of humification precursors and local bioclimatic conditions. Despite the morphological closeness in the soil profile structures of modern and MIS 5e Histic Spodic Cryosols, we may assume that the organic matter of the modern soils had relatively less time to form its molecular structure (just nearly 10 Kyr since the beginning of Holocene) than those from MIS 5, the interglacial period which spanned for nearly 30 Kyr at its warmest MIS 5e stage.

To determine the qualitative composition of HAs, an analysis using ^{13}C-NMR spectroscopy was performed. The obtained spectra are shown in Figure 3, and the results of the analysis are presented in Table 3.

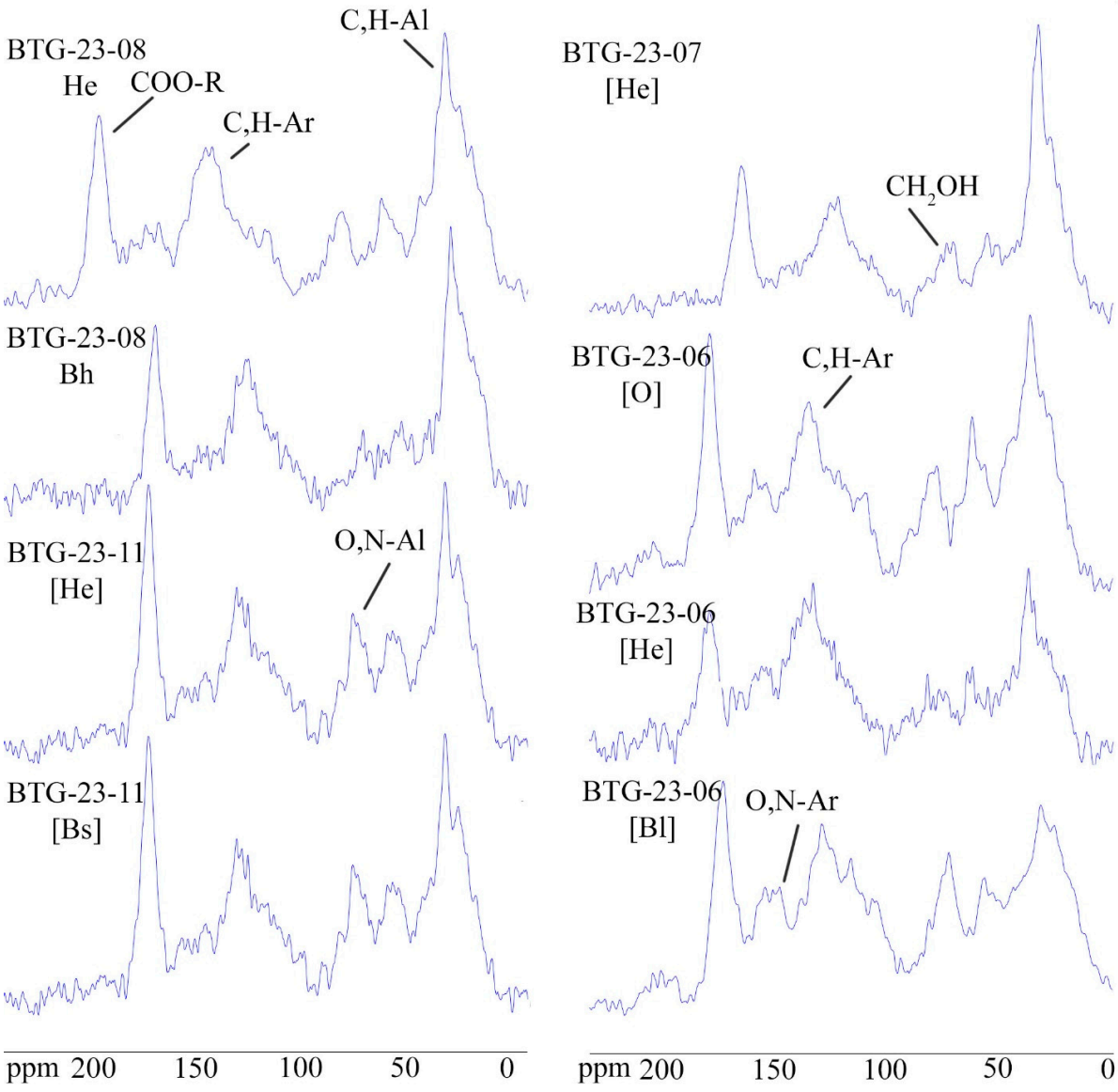

Figure 3. ^{13}C NMR spectra of HAs isolated from Cryosol and Ice Complex deposits of Batagay RTS. Soil IDs correspond to those in Table 1.

Table 3. Content of structural fragments in the studied soil samples.

ID	Horizon	Chemical Shifts, % of ^{13}C								AR *	AL **	AR/AL	AL h,r + AR h,r	C,H-AL/O,N—AL
		C,H-Al	O,N-Al	CH_2OH	C,H-Ar	O,N-Ar	COO-R	Ar=O	C=O					
1	He	32	7	15	23	8	11	1	3	32	68	0.47	55	1.45
2	Bh	35	7	12	24	7	12	1	2	32	68	0.47	59	1.84
3	[He]	29	8	17	22	7	14	1	2	30	70	0.43	51	1.16
4	[Bs]	36	7	13	22	7	12	1	2	30	70	0.43	58	1.8
5	[He]	28	8	16	23	9	12	1	3	33	67	0.49	51	1.16
6	[O]	25	6	14	29	10	12	1	3	40	60	0.67	54	1.25
7	[He]	26	7	18	24	10	11	1	3	35	65	0.54	50	1.04
8	[Bl]	28	7	16	26	9	12	1	1	36	64	0.56	54	1.21

* Aromatic structural fragments were calculated as the sum of fragments C,H-Ar, O,N-Ar and Ar=O. ** The aliphatic structural fragments were calculated as the sum of the fragments C,H-Al, O,N-Al, CH2OH, COO-R and C=O.

According to the data obtained, it was revealed that aliphatic structural fragments from 60 to 70% dominate in the HAs. The main group of aliphatic structural fragments comprises C,H-AL and O,N-AL. The content of aliphatic structural fragments is in a narrow range, which indicates a relatively homogeneous structure of HA molecules; however, we can note that the lowest content of aliphatic structural fragments is characteristic of HA molecules formed during MIS 15-17, which indicates their relatively high maturity and condensation of biodegradation-resistant molecular complexes. The highest content of aliphatic structural fragments is characteristic of the MIS 5e stage, which may indicate the formation of labile components of organic substances during the warmest phase of the deposits' formation. The content of aliphatic structural fragments at the level of 68% is observed in the HAs of modern Cryosols. This distribution of aliphatic structural fragments in HA molecules is confirmed by the elemental composition, and may indicate the presence of poorly transformed organic substances (waxes, lipids, and carbohydrates); low quinone content indicates weak oxidation of the material. The HAs of modern soils and sediments formed in MIS 5e are characterized by a relatively low degree of development of the material, while the HAs of deposits of the MIS 7 stage are characterized by a more mature structure, which may be related both to the composition of humification precursors and intramolecular transformation processes under the wet and relatively warm environmental conditions. Aromaticity (AR/AL ratio) differed significantly between MIS 15-17 (0.54–0.67) and MIS 5e/modern soils (0.43–0.49; $p < 0.01$, based on ANOVA test).

To analyze the parameters of humification and hydrophobicity of HAs, a diagram of integral indicators of HAs was constructed (Figure 4).

According to the diagram obtained, we can estimate the intramolecular processes that are currently taking place in HA molecules. Thus, it was revealed that active humification processes with the formation of hydrophobic molecular complexes occur in samples #2 (BTG-23-08 Bh) and #4 (BTG-23-11 [Bs]). These samples correspond with the zone of the most active pedogenic organomineral interaction between the superficial organogenic peaty horizon and the underlying mineral soil mass. The remaining samples are characterized by less active humification processes and the formation of hydrophobic molecules.

Principal component analysis was used for statistical analysis of the elemental and molecular composition of HAs (Figure 5).

Based on the diagrams obtained, it was found that the distribution of the studied parameters by PC1 is related to the content of the C,H-AL group due to the greatest contribution of aliphatic structural fragments to the composition of HAs. PC2 is associated with the content of C,H-AR structural fragments, which indicates a relatively high maturity of HAs formed in the Batagai RTS area as well as for modern Cryosol and Ice Complex deposits. From the ordination diagram, we can note the grouping of samples #2 and #4,

which may indicate the process of humification of organic substances with the formation of aliphatic structural fragments in the HAs.

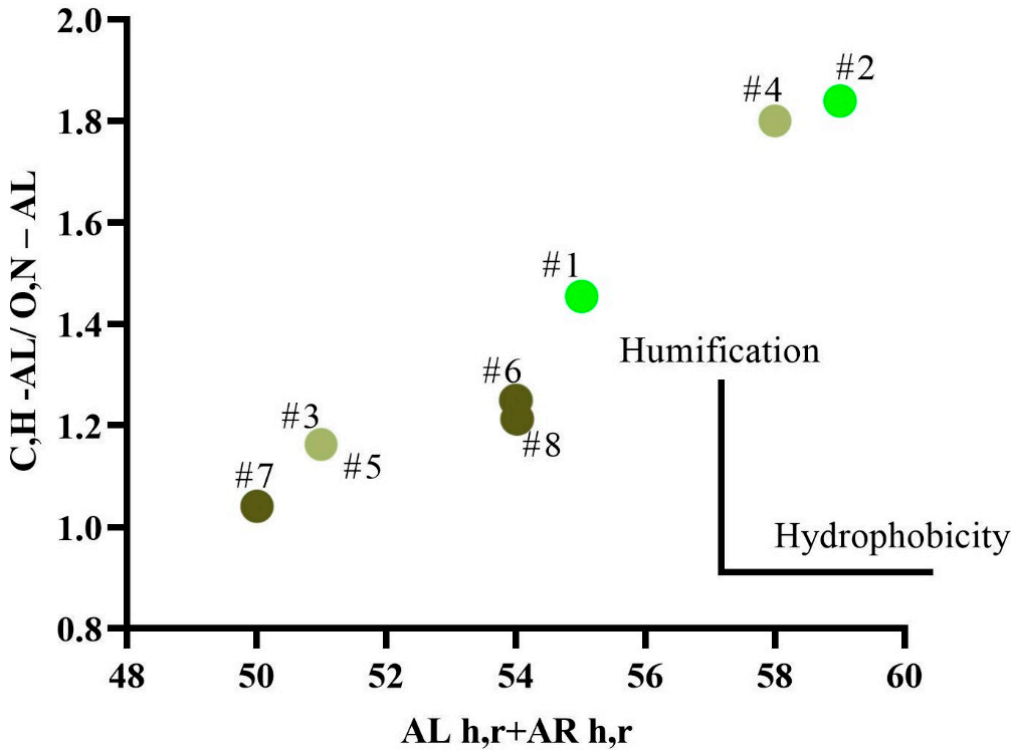

Figure 4. Diagram of integral indices of molecular composition of HAs. Soil IDs correspond to those in Table 1. Green—modern Cryosols; light-brown—MIS 5e deposits; dark-brown—MIS 7 deposits. #1–#8 correspond to Table 2.

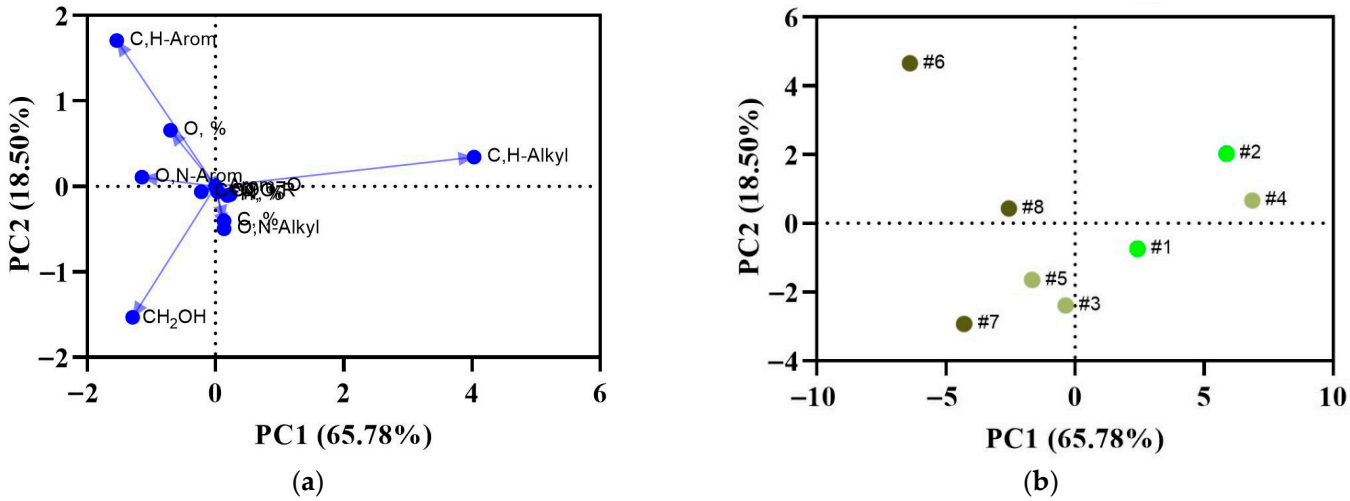

Figure 5. Results of principal component analysis for structural fragments and elemental composition of HAs. Soil IDs correspond to those in Table 1. Green—modern Cryosols; light-brown—MIS 5e deposits; dark-brown—MIS 7 deposits. (**a**)—Correlation diagram, (**b**)—Ordination diagram.

The results indicate heterogeneity in the formation of the Ice Complex (MIS 5e and MIS 7) and its organic matter composition. Organic matter from different aged paleosoils and modern Cryosols shows relatively high variability, with the highest content of biodegradation-resistant aromatic compounds found in HA samples from the oldest MIS 7 deposits. The relatively high content of aliphatic structural fragments suggests the or-

ganic material underwent limited transformation before rapid freezing [21]. HA structural analysis can reflect past climatic conditions and serve as an environmental marker [43]. Our data correlate well with HA composition studies from the Lena River Delta Ice Complex organic-rich deposits, where similarly high aromatic fragment content (up to 47%) was observed compared to modern Cryosols [42]. This suggests relatively favorable conditions of the Late Pleistocene for plant residue humification and formation of biodegradation-resistant molecular complexes. According to Murton et al. [11], MIS 7 environments likely experienced relative warming with increased landscape waterlogging, promoting pedogenesis and organic matter accumulation and transformation [21] with relatively intensive humification processes and aromatic structure formation. Organic matter transformation in waterlogged environments can produce detritus that remains relatively stable compared to biodegradation under cold conditions, as confirmed by our previous analysis of HAs of SOM from the Kolyma Lowland coastal zone [44].

Pedogenesis during the MIS 5e stage occurred under conditions similar to modern ones [35]. During this period, herbaceous phytocenoses and mixed forests likely developed, which is also reflected in the structure of HAs. Our principal component analysis revealed comparable proportions of aliphatic and aromatic structural fragments in these samples. The relatively high content of aromatic structural fragments observed in MIS 5e stage deposits (sample BTG-23-07 [He]) from an erosional incision may be attributed to the presence of charcoal particles in the organomineral material [21], which are known for their high aromatic structural fragment content. This period was characterized by widespread forest fires [45], with potential sources of charcoal particles including both aeolian transport and fluvial transportation by river waters.

The molecular composition of HAs in modern regional Cryosols is similar to those forming in soils of other regions of the Arctic [26,40], reflecting comparable bioclimatic conditions. The formation of coarse organogenic remnants results in a predominance of saturated -CH_2- groups and aliphatic structural fragments [46]. These fragments are less resistant to biodegradation and may contribute to climate change [47]. The relatively high content of aromatic structural fragments may slow the biodegradation of organic matter released from the frozen state of the Ice Complex, as these molecular complexes are more stable in the environment [47]. The molecular composition of HAs is a dynamic parameter that depends on local bioclimatic conditions and the quality of humification precursors, and may change over time. The direction of this process will depend on current environmental conditions. We suggest that over time, the content of aromatic structural fragments in HAs from thawed and redistributed MIS 7 deposits may decrease to background levels determined by local bioclimatic parameters and the quality of humification precursors.

The Batagay megaslump releases 4000–5000 tons of organic carbon annually [22], which consists of labile aliphatic-rich humic acids (MIS 5e deposits). Its rapid microbial degradation could increase CO_2 and CH_4 emissions, exacerbating Arctic warming [6,16]. Assuming a 1.5× increase in thaw rates by 2100 [8], this site alone may contribute ~6000–7500 tons C yr^{-1}, with ~30–50% emitted as CO_2/CH_4 (based on Arctic emission factors) [16]. Thawing permafrost exerts effects on hydrology, destabilizing soils and triggering thermokarst formation. This disrupts vegetation (e.g., larch woodlands) and reduces biodiversity of the region, as observed in analogous permafrost-affected regions [48]. Eroded organic matter enters rivers (Yana, Lena, Ob, Kolyma rivers), releasing bioavailable carbon that may affect the aquatic ecosystems of arctic seas [49]. Thawing of permafrost can affect the social life of the population, which is reflected in damage to infrastructure (subsidence of soil, destruction of linear objects), and threatens the food security of the peoples of the far north, as well as the release of various pathogens and pollutants stored in the permafrost [50].

4. Conclusions

The release of organic matter from the frozen state plays an important role in climate change on the planet and can serve as a marker of environmental changes in the past. The study revealed that in terms of physicochemical parameters, relict paleosoils are relatively similar in their parameters to modern analogues (carbon, nitrogen and biogenic element content), but they have significant differences in the molecular structure of HAs (AR/AL varies from 0.43 to 0.67). Analysis of the molecular composition of the different aged paleosoils from the Ice Complex deposits has shown that the initial conditions for the formation of organic matter determine their molecular structure. Thus, the HAs from MIS 7 paleosoils are characterized by a relatively high content of aromatic structural fragments, up to 40%, due to the long process of humification under the hydromorphic conditions. Organic matter in the younger paleosoils from the MIS 5e stage was characterized by a shorter stage of humification, and the formation of coniferous-deciduous forests ensured the formation of aliphatic structural fragments of up to 70%. These conditions for the formation of organic matter are quite close to those of modern soil formation; modern soils contain high percentages of aliphatic structural fragments in their organic matter, reaching up to 68%.

Based on to the obtained molecular composition data, the most active humification processes with the formation of hydrophobic molecular complexes occur in the zone of the most active pedogenic organomineral interaction between the superficial organogenic peaty horizon and the underlying mineral soil mass.

Therefore, we can conclude that local bioclimatic conditions determine the molecular composition of HAs. Aliphatic structural fragments are less resistant to biodegradation, and aliphatic-rich organic matter may be available for microbial destruction, which may affect climate change and the emission of climate-active gases into the atmosphere.

Future research should focus on investigating the transformation rates and molecular composition dynamics of HAs in SOM released from the Ice Complex for the better prediction of its contribution to global climate change.

Author Contributions: Conceptualization, V.P., E.A. and A.L.; methodology, V.P.; software, V.P.; validation A.L. and P.D.; formal analysis, V.P.; investigation, A.L. and P.D.; resources, A.L.; data curation, V.P., E.A. and A.L.; writing—original draft preparation, V.P.; writing—review and editing, V.P. and E.A.; visualization, V.P.; supervision, E.A.; project administration, E.A.; funding acquisition, E.A. All authors have read and agreed to the published version of the manuscript.

Funding: This work was supported by Saint Petersburg State University, Project No. 123042000071-8.

Data Availability Statement: The original contributions presented in this study are included in the article. Further inquiries can be directed to the corresponding author.

Acknowledgments: Center of Chemical Analyses and Materials and Center of Magnetic Resonance Research, Scientific Park of Saint-Petersburg State University. The data of NMR spectroscopy has been were obtained from the "Center of Chemical Analyses and Materials and Center of Magnetic Resonance Research".

Conflicts of Interest: The authors declare no conflicts of interest.

Abbreviations

The following abbreviations are used in this manuscript:

SOM	Soil organic matter
RTS	Retrogressive thaw slump
HAs	Humic acids
WRB	World reference base
PCA	Principal component analysis

References

1. Lal, R. Soil carbon sequestration to mitigate climate change. *Geoderma* **2004**, *123*, 1–22. [CrossRef]
2. Hugelius, G.; Strauss, J.; Zubrzycki, S.; Harden, J.W.; Schuur, E.A.G.; Ping, C.L.; Schirrmeister, L.; Grosse, G.; Michaelson, G.J.; Koven, C.D.; et al. Estimated stocks of circumpolar permafrost carbon with quantified uncertainty ranges and identified data gaps. *Biogeosciences* **2014**, *11*, 6573–6593. [CrossRef]
3. Zheng, H.; Miao, C.; Huntingford, C.; Tarolli, P.; Li, D.; Panagos, P.; Yue, Y.; Borrelli, P.; Van Oost, K. The Impacts of Erosion on the Carbon Cycle. *Rev. Geophys.* **2025**, *63*, e2023RG000829. [CrossRef]
4. Regnier, P.; Resplandy, L.; Najjar, R.G.; Ciais, P. The land-to-ocean loops of the global carbon cycle. *Nature* **2022**, *603*, 401–410. [CrossRef]
5. Zondervan, J.R.; Hilton, R.G.; Dellinger, M.; Clubb, F.J.; Roylands, T.; Ogrič, M. Rock organic carbon oxidation CO_2 release offsets silicate weathering sink. *Nature* **2023**, *623*, 329–333. [CrossRef]
6. Turetsky, M.R.; Abbott, B.W.; Jones, M.C.; Anthony, K.W.; Olefeldt, D.; Schuur, E.A.G.; Grosse, G.; Kuhry, P.; Hugelius, G.; Koven, C.; et al. Carbon release through abrupt permafrost thaw. *Nat. Geosci.* **2020**, *13*, 138–143. [CrossRef]
7. Bristol, E.M.; Behnke, M.I.; Spencer, R.G.M.; McKenna, A.; Jones, B.M.; Bull, D.L.; McClelland, J.W. Eroding Permafrost Coastlines Release Biodegradable Dissolved Organic Carbon to the Arctic Ocean. *J. Geophys. Res. Biogeosci.* **2024**, *129*, e2024JG008233. [CrossRef]
8. Nielsen, D.M.; Pieper, P.; Barkhordarian, A.; Overduin, P.; Ilyina, T.; Brovkin, V.; Baehr, J.; Dobrynin, M. Increase in Arctic coastal erosion and its sensitivity to warming in the twenty-first century. *Nat. Clim. Change* **2022**, *12*, 263–270. [CrossRef]
9. Walter Anthony, K.; Schneider von Deimling, T.; Nitze, I.; Frolking, S.; Emond, A.; Daanen, R.; Anthony, P.; Lindgren, P.; Jones, B.; Grosse, G. 21st-century modeled permafrost carbon emissions accelerated by abrupt thaw beneath lakes. *Nat. Commun.* **2018**, *9*, 3262. [CrossRef] [PubMed]
10. Tanski, G.; Bröder, L.; Wagner, D.; Knoblauch, C.; Lantuit, H.; Beer, C.; Sachs, T.; Fritz, M.; Tesi, T.; Koch, B.P.; et al. Permafrost Carbon and CO_2 Pathways Differ at Contrasting Coastal Erosion Sites in the Canadian Arctic. *Front. Earth Sci.* **2021**, *9*, 630493. [CrossRef]
11. Murton, J.B.; Edwards, M.E.; Lozhkin, A.V.; Anderson, P.M.; Savvinov, G.N.; Bakulina, N.; Bondarenko, O.V.; Cherepanova, M.V.; Danilov, P.P.; Boeskorov, V.; et al. Preliminary paleoenvironmental analysis of permafrost deposits at Batagaika megaslump, Yana Uplands, northeast Siberia. *Quat. Res.* **2017**, *87*, 314–330. [CrossRef]
12. Murton, J.; Opel, T.; Wetterich, S.; Ashastina, K.; Savvinov, G.; Danilov, P.; Boeskorov, V. Batagay megaslump: A review of the permafrost deposits, Quaternary environmental history, and recent development. *Permafr. Periglac. Process.* **2023**, *34*, 399–416. [CrossRef]
13. Strauss, J.; Schirrmeister, L.; Grosse, G.; Wetterich, S.; Ulrich, M.; Herzschuh, U.; Hubberten, H.-W. The deep permafrost carbon pool of the Yedoma region in Siberia and Alaska. *Geophys. Res. Lett.* **2013**, *40*, 6165–6170. [CrossRef]
14. Grosse, G.; Harden, J.; Turetsky, M.; McGuire, A.D.; Camill, P.; Tarnocai, C.; Frolking, S.; Schuur, E.A.G.; Jorgenson, T.; Marchenko, S.; et al. Vulnerability of high-latitude soil organic carbon in North America to disturbance. *J. Geophys. Res. Biogeosci.* **2011**, *116*. [CrossRef]
15. Strauss, J.; Schirrmeister, L.; Grosse, G.; Fortier, D.; Hugelius, G.; Knoblauch, C.; Romanovsky, V.; Schädel, C.; Schneider von Deimling, T.; Schuur, E.A.G.; et al. Deep Yedoma permafrost: A synthesis of depositional characteristics and carbon vulnerability. *Earth-Sci. Rev.* **2017**, *172*, 75–86. [CrossRef]
16. Schuur, E.A.G.; McGuire, A.D.; Schädel, C.; Grosse, G.; Harden, J.W.; Hayes, D.J.; Hugelius, G.; Koven, C.D.; Kuhry, P.; Lawrence, D.M.; et al. Climate change and the permafrost carbon feedback. *Nature* **2015**, *520*, 171–179. [CrossRef] [PubMed]
17. Knoblauch, C.; Beer, C.; Sosnin, A.; Wagner, D.; Pfeiffer, E.M. Predicting long-term carbon mineralization and trace gas production from thawing permafrost of Northeast Siberia. *Glob. Change Biol.* **2013**, *19*, 1160–1172. [CrossRef] [PubMed]
18. Kizyakov, A.I.; Wetterich, S.; Günther, F.; Opel, T.; Jongejans, L.L.; Courtin, J.; Meyer, H.; Shepelev, A.G.; Syromyatnikov, I.I.; Fedorov, A.N.; et al. Landforms and degradation pattern of the Batagay thaw slump, Northeastern Siberia. *Geomorphology* **2023**, *420*, 108501. [CrossRef]
19. Kunitsky, V.V.; Syromyatnikov, I.I.; Schirrmeister, L. Ice-rich permafrost and thermal denudation in the batagay area (Yana Upland, East Siberia). *Earth Cryosphere* **2013**, *17*, 56–68.
20. Vasil'chuk, Y.K.; Vasil'chuk, D.Y.; Ginzburg, A.P. Cryogenic soils in the area of Batagai crater in Northern Yakutia. *Arctika I. Antarkt* **2020**, *3*, 52–98.
21. Lupachev, A.V.; Tananaev, N.I.; Murton, J.B.; Kalinin, P.I.; Malyshev, V.V.; Danilov, P.P. Microstructure and geochemical properties of modern and buried soils and hosting permafrost sediments of the Batagay retrogressive thaw slump. *Quat. Res.* **2025**, *125*, 35–55. [CrossRef]

22. Kizyakov, A.I.; Korotaev, M.V.; Wetterich, S.; Opel, T.; Pravikova, N.V.; Fritz, M.; Lupachev, A.V.; Günther, F.; Shepelev, A.G.; Syromyatnikov, I.I.; et al. Characterizing Batagay megaslump topography dynamics and matter fluxes at high spatial resolution using a multidisciplinary approach of permafrost field observations, remote sensing and 3D geological modeling. *Geomorphology* **2024**, *455*, 109183. [CrossRef]
23. Serikova, S.; Pokrovsky, O.S.; Ala-Aho, P.; Kazantsev, V.; Kirpotin, S.N.; Kopysov, S.G.; Krickov, I.V.; Laudon, H.; Manasypov, R.M.; Shirokova, L.S.; et al. High riverine CO_2 emissions at the permafrost boundary of Western Siberia. *Nat. Geosci.* **2018**, *11*, 825–829. [CrossRef]
24. Lodygin, E.; Abakumov, E. The Use of Spectroscopic Methods to Study Organic Matter in Virgin and Arable Soils: A Scoping Review. *Agronomy* **2024**, *14*, 1003. [CrossRef]
25. Chukov, S.N.; Lodygin, E.D.; Abakumov, E.V. Application of 13C NMR Spectroscopy to the Study of Soil Organic Matter: A Review of Publications. *Eurasian Soil Sci.* **2018**, *51*, 889–900. [CrossRef]
26. Polyakov, V.; Abakumov, E. Assessments of Organic Carbon Stabilization Using the Spectroscopic Characteristics of Humic Acids Separated from Soils of the Lena River Delta. *Separations* **2021**, *8*, 87. [CrossRef]
27. Vasilevich, R.; Lodygin, E.; Abakumov, E. The Molecular Composition of Humic Acids in Permafrost Peats in the European Arctic as Paleorecord of the Environmental Conditions of the Holocene. *Agronomy* **2022**, *12*, 2053. [CrossRef]
28. Alekseev, I.; Abakumov, E. Soil organic carbon stocks and stability of organic matter in permafrost-affected soils of Yamal region, Russian Arctic. *Geoderma Reg.* **2022**, *28*, e00454. [CrossRef]
29. Murton, J.B.; Opel, T.; Toms, P.; Blinov, A.; Fuchs, M.; Wood, J.; Gärtner, A.; Merchel, S.; Rugel, G.; Savvinov, G.; et al. A multimethod dating study of ancient permafrost, Batagay megaslump, east Siberia. *Quat. Res.* **2021**, *105*, 1–22. [CrossRef]
30. Günther, F.; Grosse, G.; Jones, B.M.; Schirrmeister, L.; Romanovsky, V.E.; Kunitsky, V.V. Unprecedented permafrost thaw dynamics on a decadal time scale: Batagay mega thaw slump development, Yana Uplands, Yakutia, Russia. In Proceedings of the AGU Fall Meeting, San Francisco, CA, USA, 12–16 December 2016; p. 12.
31. Savvinov, G.N.; Danilov, P.P.; Petrov, A.A. Environmental Problems of the Verkhoyansky Region. *Vestn. North-East. Fed. Univ.* **2018**, *6*, 18–33.
32. Gavrilov, A.V. *Yano-Oymyakonskiy Region. Geocryology of USSR, Eastern Siberia and Far East*; Nedra: Moscow, Russia, 1989.
33. Shestakova, A.A.; Fedorov, A.N.; Torgovkin, Y.I.; Konstantinov, P.Y.; Vasyliev, N.F.; Kalinicheva, S.V.; Samsonova, V.V.; Hiyama, T.; Iijima, Y.; Park, H.; et al. Mapping the Main Characteristics of Permafrost on the Basis of a Permafrost-Landscape Map of Yakutia Using GIS. *Land* **2021**, *10*, 462. [CrossRef]
34. Isaev, A.P.; Protopopov, A.V.; Protopopova, V.V.; Egorova, A.A.; Timofeyev, P.A.; Nikolaev, A.N.; Shurduk, I.F.; Lytkina, L.P.; Ermakov, N.B.; Nikitina, N.V.; et al. Vegetation of Yakutia: Elements of Ecology and Plant Sociology. In *The Far North: Plant Biodiversity and Ecology of Yakutia*; Troeva, E.I., Isaev, A.P., Cherosov, M.M., Karpov, N.S., Eds.; Springer: Dordrecht, The Netherlands, 2010; pp. 143–260.
35. Ashastina, K.; Kuzmina, S.; Rudaya, N.; Troeva, E.; Schoch, W.H.; Römermann, C.; Reinecke, J.; Otte, V.; Savvinov, G.; Wesche, K.; et al. Woodlands and steppes: Pleistocene vegetation in Yakutia's most continental part recorded in the Batagay permafrost sequence. *Quat. Sci. Rev.* **2018**, *196*, 38–61. [CrossRef]
36. IUSS Working Group WRB. *World Reference Base for Soil Resources. International Soil Classification System for Naming Soils and Creating Legends for Soil Maps*, 4th ed.; International Union of Soil Sciences (IUSS): Vienna, Austria, 2022; p. 234.
37. Gubin, S.V. Late Pleistocene pedogenesis on the territory of North-East Eurasia. *Dokl. Akad. Nauk. SSSR* **1996**, *351*, 544–547.
38. Gubin, S.V. Pedogenesis as the element of the formation mechanism of the Late Pleistocene Ice Complex. *Earth's Cryosphere* **2002**, *6*, 82–91.
39. Vorobyova, L.A. *Theory and Practice of Chemical Analysis of Soils*; GEOS: Moscow, Russia, 2006; p. 400.
40. Vasilevich, R.S.; Beznosikov, V.A.; Lodygin, E.D. Molecular Structure of Humus Substances in Permafrost Peat Mounds in Forest-Tundra. *Eurasian Soil Sci.* **2019**, *52*, 283–295. [CrossRef]
41. Schädel, C.; Schuur, E.A.G.; Bracho, R.; Elberling, B.; Knoblauch, C.; Lee, H.; Luo, Y.; Shaver, G.R.; Turetsky, M.R. Circumpolar assessment of permafrost C quality and its vulnerability over time using long-term incubation data. *Glob. Change Biol.* **2014**, *20*, 641–652. [CrossRef] [PubMed]
42. Polyakov, V.; Orlova, K.; Abakumov, E. Soils of the Lena River Delta, Yakutia, Russia: Diversity, Characteristics and Humic Acids Molecular Composition. *Polarforschung* **2018**, *88*, 135–150.
43. Dergacheva, M.I.; Nekrasova, O.A.; Okoneshnikova, M.V.; Vasileva, D.I.; Gavrilov, D.A.; Ochur, K.O.; Ondar, E.E. Ratio of elements in humic acids as a source of information on the environment of soil formation. *Contemp. Probl. Ecol.* **2012**, *5*, 497–504. [CrossRef]
44. Polyakov, V.; Lupachev, A.; Gubin, S.; Abakumov, E. Soil Organic Matter of Tidal Marsh Permafrost-Affected Soils of Kolyma Lowland. *Agronomy* **2023**, *13*, 48. [CrossRef]
45. Sycheva, S.A.; Anisyutkin, N.K.; Khokhlova, O.S.; Pushkina, P.R.; Ukrainsky, P.A. Paleoecology of a Multilayered Early Paleolithic Site Bairaki in Transnistria. *Izv. Ross. Akad. Nauk. Seriâ Geogr.* **2023**, *87*, 1238–1257. [CrossRef]

46. Chen, J.; Gu, B.; LeBoeuf, E.J.; Pan, H.; Dai, S. Spectroscopic characterization of the structural and functional properties of natural organic matter fractions. *Chemosphere* **2002**, *48*, 59–68. [CrossRef] [PubMed]
47. Semenov, V.M.; Ivannikov, L.A.; Tulina, A.S. Stabilization of organic matter in the soil. *Agrochimia* **2009**, *10*, 77–96.
48. Jin, X.-Y.; Jin, H.-J.; Iwahana, G.; Marchenko, S.S.; Luo, D.-L.; Li, X.-Y.; Liang, S.-H. Impacts of climate-induced permafrost degradation on vegetation: A review. *Adv. Clim. Change Res.* **2021**, *12*, 29–47. [CrossRef]
49. O'Donnell, J.A.; Carey, M.P.; Koch, J.C.; Baughman, C.; Hill, K.; Zimmerman, C.E.; Sullivan, P.F.; Dial, R.; Lyons, T.; Cooper, D.J.; et al. Metal mobilization from thawing permafrost to aquatic ecosystems is driving rusting of Arctic streams. *Commun. Earth Environ.* **2024**, *5*, 268. [CrossRef]
50. Revich, B.A.; Eliseev, D.O.; Shaposhnikov, D.A. Risks for Public Health and Social Infrastructure in Russian Arctic under Climate Change and Permafrost Degradation. *Atmosphere* **2022**, *13*, 532. [CrossRef]

Disclaimer/Publisher's Note: The statements, opinions and data contained in all publications are solely those of the individual author(s) and contributor(s) and not of MDPI and/or the editor(s). MDPI and/or the editor(s) disclaim responsibility for any injury to people or property resulting from any ideas, methods, instructions or products referred to in the content.